Suppression of magnetoelectric effects in DyCrO$_4$ by chemical doping ⊘

Xudong Shen; Long Zhou; Xubin Ye; Zhehong Liu; Guangxiu Liu; Shijun Qin; Jia Guo; Lei Gao; Yisheng Chai; Youwen Long ✉ 📧

Check for updates

View Online

Export Citation

16 April 2024 10:20:16

Suppression of magnetoelectric effects in DyCrO$_4$ by chemical doping

View Online   Export Citation   CrossMark

Xudong Shen,[1,2] Long Zhou,[1,2] Xubin Ye,[1,2] Zhehong Liu,[1,2] Guangxiu Liu,[1,2] Shijun Qin,[1,2] Jia Guo,[1,2] Lei Gao,[1,2] Yisheng Chai,[3] and Youwen Long[1,2,4,a)] (iD)

AFFILIATIONS

[1] Beijing National Laboratory for Condensed Matter Physics, Institute of Physics, Chinese Academy of Sciences, Beijing 100190, China

[2] School of Physics, University of Chinese Academy of Sciences, Beijing 100049, China

[3] Low Temperature Physics Laboratory, College of Physics, and Center of Quantum Materials and Devices, Chongqing University, Chongqing 401331, China

[4] Songshan Lake Materials Laboratory, Dongguan, Guangdong 523808, China

[a)] Author to whom correspondence should be addressed: ywlong@iphy.ac.cn

ABSTRACT

The scheelite-type DyCrO$_4$ shows a large linear magnetoelectric effect and field-induced ferromagnetism and ferroelectricity. In this article, we investigate the Bi-doping effects on the crystal structure, magnetism, dielectric constant, and electric polarization for a Dy$_{1-x}$Bi$_x$CrO$_4$ ($x = 0$, 0.05, 0.1) solid solution. The substitution of Bi for Dy up to 10% does not change the structure and antiferromagnetic ordering temperature very much. However, it remarkably suppresses the magnetodielectric effect from 14% in the parent phase to 3.2% in the $x = 0.1$ sample. More sharply, the maximum field-induced electric polarization is reduced from 320 μC/m^2 ($x = 0$) to 10 μC/m^2 ($x = 0.1$). The results reveal that Dy plays a crucial role in the origin of the large linear magnetoelectric effect of DyCrO$_4$, so chemical doping on this site provides an effective method to manipulate the magnetodielectric and magnetoelectric properties.

Published under license by AIP Publishing. https://doi.org/10.1063/1.5140505

The magnetoelectric (ME) effect, which indicates electric polarization (P) produced by a magnetic field (H) or magnetization (M) yielded by an electric field (E), has been studied widely since the first discovery of the linear ME property of Cr$_2$O$_3$ in theory[1] and experiments.[2] In spite of numerous investigations, the linear ME coefficient α, which is defined by the expression $P = \alpha H$ based on the differentiation of free energy, is still limited below 30 ps/m in most compounds.[3] Although some type-II multiferroics show huge ME coupling effects, they only occur around the phase transitions and drastically decrease to nearly naught away from the critical temperatures or fields.[4–6] It is therefore, for practical applications such as in spintronic and memory devices, a pressing need to find new materials with larger ME coefficients in wider temperature and/or field ranges. In principle, the upper bound of α is proportional to the geometric mean of magnetic and electric susceptibilities.[7] Thus, ferromagnetic ferroelectrics are promising candidates for exploring giant ME effects. Unfortunately, such kind of materials are rare and yet to be known.

The RCrO$_4$ (R = rare earth) family used to be a desirable system to study the intriguing magnetic properties arising from $3d$-$4f$ magnetic interactions and intrinsic rare earth anisotropy.[8–14] At ambient conditions, most RCrO$_4$ oxides crystallize into a tetragonal zircon-type phase with space group $I4_1/amd$. In this symmetry, the CrO$_4$ tetrahedra and RO$_8$ dodecahedra are alternately arranged along the c-axis, while the edge-sharing RO$_8$ dodecahedra are aligned along the a-axis [see the supplementary material Fig. S1(a)]. Since there exist a large number of structural cavities under higher pressure, the zircon phase often changes into a scheelite-type structure irreversibly, accompanied by a sharp volume reduction by about 10%. The crystal constitution of the scheelite-type phase with space group $I4_1/a$ is shown in the supplementary material Fig. S1(b). It is formed by chains of alternate corner-sharing CrO$_4$ tetrahedra and RO$_8$ dodecahedra along the a-axis, and two RO$_8$ dodecahedra are connected by sharing edges along the c-axis. Since the R-O-Cr superexchange pathways vary significantly, the zircon and scheelite phases exhibit essentially different magnetic properties.[15] For example, a long-range ferromagnetic (FM) phase transition is found to occur in the zircon-type DyCrO$_4$, whereas the scheelite phase displays antiferromagnetic (AFM) ordering.[16] Unexpectedly, we recently found that the scheelite-type DyCrO$_4$ shows a large linear ME effect with a coupling coefficient α as large as 50 ps/m in a wider magnetic field region from -3 T to 3 T.[17] More

16 April 2024 10:20:16

interestingly, a higher magnetic field (>3.1 T) can induce a metamagnetic transition from the initially collinear AFM structure to a canted one with a giant magnetic moment up to 7.1 μ_B/f.u. The new spin structure can break the space inversion symmetry and therefore induce spontaneous ferroelectric polarization, giving rise to the presence of ferromagnetism and ferroelectricity.

Chemical doping is an effective method to tune physical properties. For example, in the multiferroic material TbMnO$_3$,[18] the A-site doping of Bi for Tb considerably suppresses the spin ordering of the Tb^{3+}-magnetic sublattice and thereby reduces the ferroelectric ordering temperature.[19,20] In contrast, a slight Al-doping in DyMnO$_3$ can enhance the polarization.[21] By means of Bi substitution in hexaferrite SrFe$_{12}$O$_{19}$, the ME coupling has been strengthened, and the lattice is highly strained.[22] As far as the scheelite-type DyCrO$_4$ is concerned, both Dy^{3+} and Cr^{5+} ions take part in the spin ordering and contribute to the large linear ME behavior. It is therefore interesting to study the chemical doping effects on the magnetoelectric properties. In this paper, a small amount of Bi is used to replace Dy. The related variations in the structure, magnetism, dielectric constant, and ferroelectric polarization are studied in detail.

The specific sample synthesis and measurement methods used in this work are presented in the supplementary material. The XRD patterns of Dy$_{1-x}$Bi$_x$CrO$_4$ prepared at ambient pressure with $x = 0$, 0.05, and 0.1 are shown in the supplementary material Fig. S1(c). All the peaks can be indexed on the basis of a zircon-type tetragonal structure with space group $I4_1/amd$ (No. 141). After high-pressure treatment, the XRD patterns experience essential variations. Correspondingly, a tetragonal scheelite-type structure in a $I4_1/a$ symmetry (No. 88) can fit the patterns very well. No impurity is discernable from XRD data in both the zircon and scheelite phases. Since the effective ionic radius of Bi^{3+} is larger than that of Dy^{3+},[23] with increasing substitution of Bi in Dy$_{1-x}$Bi$_x$CrO$_4$, the diffraction peaks in both phases systematically shift toward lower angles [see the supplementary material Figs. S1(c) and S1(d)], suggesting that Bi and Dy form a solid solution at the same Wyckoff position. By comparison, in the scheelite-type samples with $x = 0$ and 0.1, the lattice parameters just slightly change from $a = 5.015$ to 5.023 Å, and $c = 11.311$ to 11.320 Å. Note that in our attempts, the maximum doping level of Bi for Dy is $x = 0.1$, above which considerable impurity phases emerge.

Since the magnetic ion of Dy^{3+} is in portion replaced by the non-magnetic Bi^{3+}, the magnetism of the scheelite-type Dy$_{1-x}$Bi$_x$CrO$_4$ solid solution is studied by magnetic susceptibility (χ), magnetization, and specific heat (C_p). Figure 1(a) shows the temperature dependence of χ measured at 100 Oe in a field-cooling mode. As previously reported[17] and shown in Fig. 1(a), the parent compound DyCrO$_4$ experiences an AFM phase transition at $T_N \sim 24$ K, following by an upturn at lower temperatures. A similar susceptibility behavior is found to occur in the $x = 0.05$ sample, but the T_N slightly decreases to a lower temperature (see the inset). Although the low-temperature upturn is enhanced in the $x = 0.1$ sample, an AFM kink can still be distinguished. To determine the AFM ordering temperatures more precisely, temperature dependent C_p was measured under the zero field condition. As shown in Fig. 1(b), all three compositions display sharp λ-type anomalies in specific heat. According to the peak positions, the T_N is assigned to be 24 K for DyCrO$_4$, while Dy$_{0.95}$Bi$_{0.05}$CrO$_4$ and Dy$_{0.9}$Bi$_{0.1}$CrO$_4$ have a comparable T_N of about 22 K. Therefore, the Bi doping with the
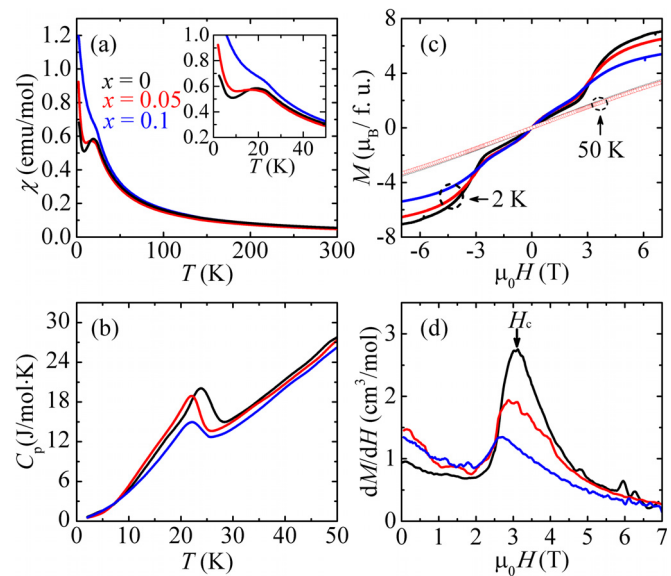
FIG. 1. Temperature dependence of (a) magnetic susceptibility measured at 100 Oe and (b) specific heat measured at zero field. (c) Magnetization as a function of field at 2 K and 50 K, and (d) its derivative at 2 K for scheelite-type Dy$_{1-x}$Bi$_x$CrO$_4$. The inset of (a) is an enlarged view for the AFM transitions.

content $\leq 10\%$ does not change the long-range AFM ordering temperature too much.

The field dependence of isothermal magnetization curves for these three samples is presented in Fig. 1(c). Above the T_N (e.g., at 50 K), the magnetization exhibits a good linear relationship with the magnetic field, in agreement with the paramagnetic behavior. As expected for the long-range AFM ordering, linear magnetization behaviors are also observed at 2 K under lower fields such as below 3 T for DyCrO$_4$. When a higher magnetic field is applied, however, metamagnetic transitions are found to occur in all three samples, giving rise to large FM components. Specifically, the magnetic moments measured at 7 T and 2 K are 7.1 μ_B/f.u. for DyCrO$_4$, 6.5 μ_B/f.u. for Dy$_{0.95}$Bi$_{0.05}$CrO$_4$, and 5.4 μ_B/f.u. for Dy$_{0.9}$Bi$_{0.1}$CrO$_4$. Based on the field derivative of magnetization, the metamagnetic transition critical field is determined to be $H_C = 3.1$ T for DyCrO$_4$, 2.93 T for Dy$_{0.95}$Bi$_{0.05}$CrO$_4$, and 2.67 T for Dy$_{0.9}$Bi$_{0.1}$CrO$_4$ [see Fig. 1(d)]. The gradually decreased magnetic moment and critical field are attributed to the increasing substitution of Dy^{3+} by nonmagnetic Bi^{3+}. This behavior is similar with that reported in another Bi-substituted solid solution of Dy$_{1-x}$Bi$_x$MnO$_3$.[24] The field dependent neutron diffraction in DyCrO$_4$ indicates that a higher magnetic field can change the initially collinear AFM structure to a canted one, which leads to the metamagnetic transition as well as the large FM component.[17] Similar variations should take place in the Bi-doped Dy$_{0.95}$Bi$_{0.05}$CrO$_4$ and Dy$_{0.9}$Bi$_{0.1}$CrO$_4$. Note that the field-induced metamagnetic transition is also reported in the zircon-type DyVO$_4$,[25] DyPO$_4$,[26] and perovskite-type DyAlO$_3$,[27] in which 4f-Dy^{3+} is the only magnetic ion. This suggests that Dy^{3+} may play a dominant role in the metamagnetic transitions in our samples. At the ground state, the scheelite-type DyCrO$_4$ has a collinear AFM structure with a magnetic point group of $2'/m$.[17,28] The related ME tensor allows to generate a linear ME effect.

Moreover, once the metamagnetic transition takes place, the new spin structure can break the space inversion symmetry and thereby induces spontaneous ferroelectric polarization. It is therefore interesting to study the dielectric and ferroelectric properties of the $Dy_{1-x}Bi_xCrO_4$ solid solution. Figures 2(a)–2(c) show the temperature dependent relative dielectric constant measured at 1 MHz with magnetic fields varying from 0 to 9 T for $DyCrO_4$, $Dy_{0.95}Bi_{0.05}CrO_4$, and $Dy_{0.9}Bi_{0.1}CrO_4$, respectively. At zero field, all the dielectric constant curves smoothly change with temperature and there are no anomalies around T_N. When a magnetic field is applied, however, sharp dielectric peaks are found to occur near the AFM transition temperatures in these three samples. Moreover, with the increasing field, the induced dielectric peaks become sharper and slightly shift toward lower temperatures. On the other hand, at a fixed field such as 4 T to measure the dielectric constant using different frequencies, one finds that the dielectric peak is almost frequency independent (see the supplementary material Fig. S2). These observations suggest that the magnetic field may induce intrinsic electric polarization in $Dy_{1-x}Bi_xCrO_4$, i.e., the linear ME effect occurs in this solid solution. Although the Bi-doped samples show a similar field dependent dielectric feature with that of the parent $DyCrO_4$, the magnitude of variation in the dielectric constant is closely related to the content of Bi. To characterize the magnetodielectric (MD) effect, an MD coefficient is calculated by the equation MD $(\%) = \{[\varepsilon_r\ (\mu_0H)\ -\ \varepsilon_r\ (0)]/\varepsilon_r\ (0)\} \times\ 100\%$ as presented in Figs. 2(d)–2(f). For instance, at 9 T, the maximum MD values observed in both $DyCrO_4$ and $Dy_{0.95}Bi_{0.05}CrO_4$ are close to 14%. However, they are drastically reduced to about 3% in the $x = 0.1$ sample, accompanied by a broadening of the dielectric and MD peaks. Therefore,
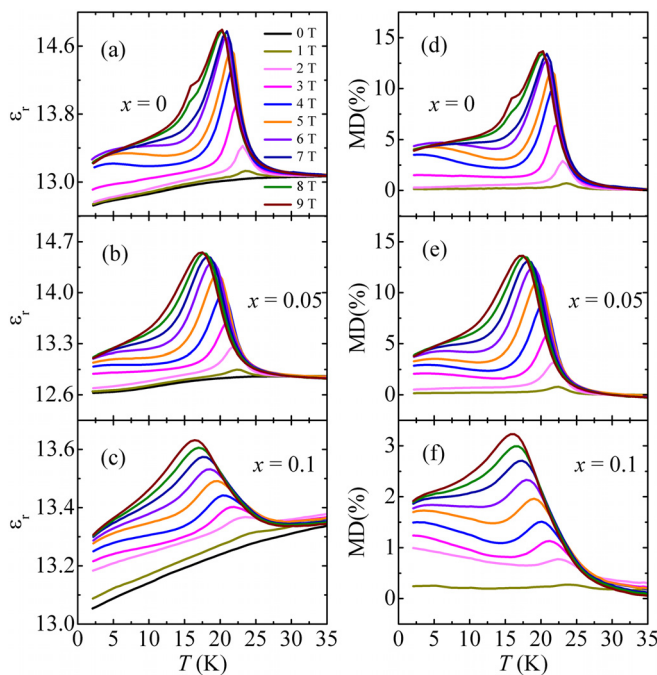
although the AFM phase transition temperature does not change much in $Dy_{1-x}Bi_xCrO_4$, the MD effect varies considerably by Bi-doping only up to 10%.

To get a deeper insight into the effect of Bi substitution on ferroelectric properties, the temperature dependence of pyroelectric current was measured at different magnetic fields after poling with electric fields of $+E$ ($= 1$ MV/m) and $–E$. By integrating the current as a function of time, the temperature dependent electric polarization under different fields is obtained, as shown in Figs. 3(a)–3(c). Similarly with the dielectric measurements, one cannot find any detectable electric polarization at zero field (not shown here). However, applying a magnetic field can induce the presence of polarization below T_N. Moreover, both the sign and magnitude of polarization are completely reversible if the poling electric field is reversed, confirming the intrinsic linear ME effects in the $Dy_{1-x}Bi_xCrO_4$ system. Different from the induced dielectric peaks, which are always enhanced by the increasing field (see Fig. 2), the induced polarization reaches a saturation value with the field up to about 4 T. Above this field, the magnitude of polarization decreases slightly with an increasing magnetic field. To reveal such a tendency, we compare the polarization measured at 10 K under various fields for three samples, as shown in Fig. 3(d). One finds that the polarization is reduced from 320 $\mu C/m^2$ in $DyCrO_4$ to 150 $\mu C/m^2$ in $Dy_{0.95}Bi_{0.05}CrO_4$ and then to 10 $\mu C/m^2$ in $Dy_{0.9}Bi_{0.1}CrO_4$ at 4 T. It means that Bi-10% doping can strongly suppress the polarization as well as the linear ME effect by two orders of magnitude.

As observed in the current $Dy_{1-x}Bi_xCrO_4$, a similar suppression of electric polarization was reported in $TbMn_{1-x}Ru_xO_3$ ($x = 0 – 0.1$)[29] and $TbMn_{1-x}Cr_xO_3$ ($x = 0 – 0.04$)[30] solid solutions with slight B-site doping. In these two compounds, the substituted Ru/Cr ions can break the initial spiral spin structure composed of Mn ions, which are responsible for the formation of spin-induced ferroelectricity. As a result, the polarization is suppressed to a large degree. In $DyCrO_4$, both Dy^{3+} and Cr^{5+} ions contribute to the AFM ordering. Moreover,

FIG. 2. Temperature dependences of (a)–(c) relative dielectric constant ε_r and (d)–(f) magnetodielectric effect coefficient magnetodielectric (MD) for scheelite-type $Dy_{1-x}Bi_xCrO_4$.
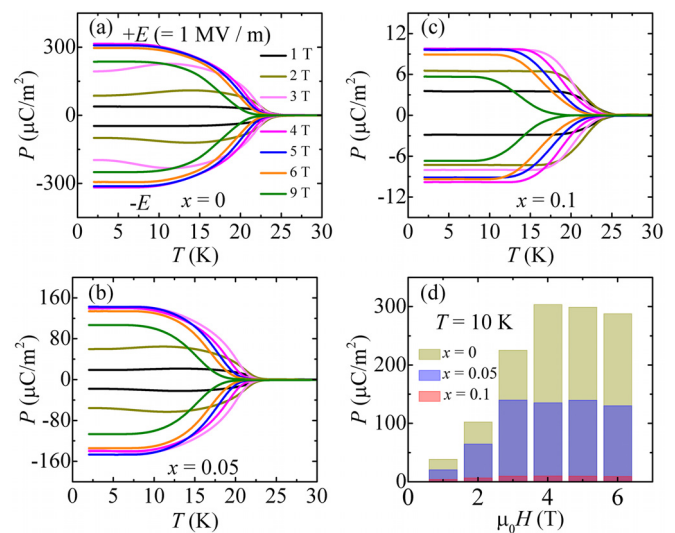
FIG. 3. Temperature dependences of electric polarization measured at different fields with (a) $x = 0$, (b) $x = 0.05$, and (c) $x = 0.1$ for scheelite-type $Dy_{1-x}Bi_xCrO_4$. (d) Comparison of polarization measured at 10 K and various magnetic fields.

Dy^{3+} has a much larger local moment than that of Cr^{5+}. Once the Dy^{3+} is replaced by a nonmagnetic Bi^{3+}, it will affect the Dy^{3+}-O-Cr^{5+} superexchange interactions and therefore decreases the field-induced electric polarization greatly. As is well known, the $6s^2$ lone-pair electrons of Bi^{3+} have remarkable stereochemical activity to form covalent bonds with O-2p electrons along one special direction and thus induce off-centering distortion in the presence of ferroelectric relaxor behavior.[31–33] This kind of stereochemical effect is responsible for the enhancement of electric polarization in the Bi-doped $La_{0.9}Bi_{0.1}AlO_3$.[34] In the current $Dy_{1-x}Bi_xCrO_4$ solid solution with x up to 0.1, however, one cannot find any ferroelectric relaxor behavior as featured by the frequency independent dielectric peaks shown in Fig. S2. Besides, no structural distortion from the centrosymmetric $I4_1/a$ space group to a polar one is found to occur. It means that Bi occupies the center position in Dy/BiO_8 dodecahedra without a detectable off-centering distortion. Therefore, the stereochemical activity of Bi^{3+} is absent in $Dy_{1-x}Bi_xCrO_4$. The Bi-doping in this solid solution thus mainly tends to destroy the AFM superexchange pathways as well as the related spin structure, giving rise to a sharp suppression of magnetodielectric and magnetoelectric effects.

In summary, we performed partial substitution of Bi for Dy in $DyCrO_4$. By high-pressure treatment of the zircon-type precursors, a scheelite-type $Dy_{1-x}Bi_xCrO_4$ solid solution with a space group of $I4_1/a$ was obtained. The maximum Bi doping in this study is $x = 0.1$. As the x increases, the lattice parameters expand slightly due to the larger ionic radius of Bi^{3+} than that of Dy^{3+}. In magnetism, all the compositions show long-range AFM transitions. At higher fields, they experience metamagnetic transitions in the presence of large FM components. The magnetic moment and critical field are found to be inversely proportional to the Bi content. Magnetic field induced dielectric peaks and electric polarization are observed in this solid solution, suggesting the remarkable linear ME behavior. Although the AFM transition temperature is little dependent on Bi substitution, both the MD and ME effects are sharply reduced by the introduction of Bi. In particular, the field induced electric polarization decreases by two orders of magnitude from $x = 0$ to 0.1. Therefore, the Dy^{3+} ions play a crucial role in the magnetoelectric properties of $Dy_{1-x}Bi_xCrO_4$, making chemical doping a highly efficient method to tune the linear ME effect and field-induced ferromagnetism and ferroelectricity.

See the supplementary material for the experimental details, the crystal structures and XRD patterns for zircon and scheelite $Dy_{1-x}Bi_xCrO_4$ (Fig. S1), and the temperature dependences of the relative dielectric constant measured at 4 T and different frequencies (Fig. S2).

REFERENCES

[1] I. E. Dzyaloshinskii, Sov. Phys. JETP **10**, 628 (1960).
[2] D. N. Astrov, Sov. Phys. JETP **11**, 708 (1960).
[3] M. Fiebig, J. Phys. D: Appl. Phys. **38**, R123 (2005).
[4] K. Zhai, Y. Wu, S. Shen, W. Tian, H. Cao, Y. Chai, B. C. Chakoumakos, D. Shang, L. Yan, F. Wang, and Y. Sun, Nat. Commun. **8**, 519 (2017).
[5] Y. S. Oh, S. Artyukhin, J. J. Yang, V. Zapf, J. W. Kim, D. Vanderbilt, and S. W. Cheong, Nat. Commun. **5**, 3201 (2014).
[6] Y. Wang, G. L. Pascut, B. Gao, T. A. Tyson, K. Haule, V. Kiryukhin, and S. W. Cheong, Sci. Rep. **5**, 12268 (2015).
[7] W. F. Brown, R. M. Hornreich, and S. Shtrikman, Phys. Rev. **168**, 574 (1968).
[8] E. Jiménez, J. Isasi, and R. Sáez-Puche, J. Solid State Chem. **164**, 313 (2002).
[9] E. Jiménez, J. Isasi, and R. Sáez-Puche, J. Alloy. Compd. **312**, 53 (2000).
[10] R. Sáez-Puche, E. Jiménez, J. Isasi, M. T. Fernández-Díaz, and J. L. García-Muñoz, J. Solid State Chem. **171**, 161 (2003).
[11] R. Sáez Puche, E. Climent, M. G. Rabie, J. Romero, and J. M. Gallardo, J. Phys.: Conf. Ser. **325**, 012012 (2011).
[12] A. J. Dos santos-García, E. Climent-Pascual, J. M. Gallardo-Amores, M. G. Rabie, Y. Doi, J. Romero de Paz, B. Beuneu, and R. Sáez-Puche, J. Solid State Chem. **194**, 119 (2012).
[13] Y. W. Long, Q. Huang, L. X. Yang, Y. Yu, Y. X. Lv, J. W. Lynn, Y. Chen, and C. Q. Jin, J. Magn. Magn. Mater. **322**, 1912 (2010).
[14] A. Midya, N. Khan, D. Bhoi, and P. Mandal, Appl. Phys. Lett. **103**, 092402 (2013).
[15] E. Climent Pascual, J. M. Gallardo Amores, R. Sáez Puche, M. Castro, N. Taira, J. Romero de Paz, and L. C. Chapon, Phys. Rev. B **81**, 174419 (2010).
[16] Y. W. Long, Q. Q. Liu, Y. X. Lv, R. C. Yu, and C. Q. Jin, Phys. Rev. B **83**, 024416 (2011).
[17] X. D. Shen, L. Zhou, Y. S. Chai, Y. Wu, Z. H. Liu, Y. Y. Yin, H. B. Cao, C. Cruz, Y. Sun, C. Q. Jin, A. Muñoz, J. A. Alonso, and Y. W. Long, NPG Asia Mater. **11**, 50 (2019).
[18] T. Kimura, T. Goto, H. Shintani, K. Ishizaka, T. Arima, and Y. Tokura, Nature **426**, 55 (2003).
[19] C. Zhang, H. T. Yan, X. F. Wang, D. W. Kang, L. B. Li, X. M. Lu, and J. S. Zhu, Mater. Lett. **111**, 147 (2013).
[20] I. V. Golosovsky, A. A. Mukhin, V. Y. Ivanov, S. B. Vakhrushev, E. I. Golovenchits, V. A. Sanina, J. U. Hoffmann, R. Feyerherm, and E. Dudzik, Eur. Phys. J. B **85**, 103 (2012).
[21] N. Zhang, K. F. Wang, S. J. Luo, T. Wei, X. W. Dong, S. Z. Li, J. G. Wan, and J. M. Liu, Appl. Phys. Lett. **96**, 252902 (2010).
[22] M. R. Sahoo, A. Barik, S. Kuila, S. Tiwary, and P. N. Vishwakarma, J. Appl. Phys. **126**, 074104 (2019).
[23] R. D. Shannon, Acta Crystallogr., Sect. A **32**, 751 (1976).
[24] K. Yadagiri, R. Nithya, N. Shukla, and A. T. Satya, J. Alloys Compd. **695**, 2959 (2017).
[25] A. Midya, N. Khan, D. Bhoi, and P. Mandal, Physica B **448**, 43 (2014).
[26] G. T. Rado, Phys. Rev. Lett. **23**, 644 (1969).
[27] L. M. Holmes, L. G. Van Uitert, R. R. Hecker, and G. W. Hull, Phys. Rev. B **5**, 138 (1972).
[28] A. J. Dos santos-García, E. Climent-Pascual, M. G. Rabie, J. Romero de Paz, J. M. Gallardo Amores, D. Khalyavin, and R. Sáez-Puche, J. Phys.: Conf. Ser. **549**, 012021 (2014).
[29] Y. Y. Guo, Y. J. Guo, N. Zhang, L. Lin, and J. M. Liu, Appl. Phys. A **106**, 113 (2012).
[30] Y. Y. Guo, Y. L. Wang, J. M. Liu, and T. Wei, J. Appl. Phys. **116**, 063905 (2014).
[31] R. Seshadri and N. A. Hill, Chem. Mater. **13**, 2892 (2001).
[32] L. Q. Zhou, P. M. Vilarinho, and J. L. Baptista, J. Eur. Ceram. Soc. **21**, 531 (2001).
[33] N. E. Rajeevan, P. P. Pradyumnan, R. Kumar, D. K. Shukla, S. Kumar, A. K. Singh, S. Patnaik, S. K. Arora, and I. V. Shvets, Appl. Phys. Lett. **92**, 102910 (2008).
[34] M. J. Si, Y. D. Hou, H. Y. Ge, M. K. Zhu, and H. Yan, J. Appl. Phys. **110**, 094107 (2011).

16 April 2024 10:20:16